ANTIOXIDANTS & REDOX SIGNALING
Volume 9, Number 11, 2007

DOI: 10.1089/ars.2007.1693

Original Research Communication

Mitochondrial Redox Cycling of Mitoquinone Leads to Superoxide Production and Cellular Apoptosis

ABDULRAHMAN K. DOUGHAN and SERGEY I. DIKALOV

ABSTRACT

The mitochondria-targeted drug mitoquinone (MitoQ) has been used as an antioxidant that may selectively block mitochondrial oxidative damage; however, it has been recently suggested to increase reactive oxygen species (ROS) generation in malate- and glutamate-fueled mitochondria. To address this controversy, we studied the effects of MitoQ on endothelial and mitochondrial ROS production. We found that in a cell-free system with flavin-containing enzyme cytochrome P-450 reductase, MitoQ is a very efficient redox cycling agent and produced more superoxide compared with equal concentrations of menadione (10–1,000 n*M*). Treatment of endothelial cells with MitoQ resulted in a dramatic increase in superoxide production. In isolated mitochondria, MitoQ increased complex I–driven mitochondrial ROS production, whereas supplementation with ubiquinone-10 had no effect on ROS production. Similar results were observed in mitochondria isolated from endothelial cells incubated for 1 h with MitoQ. Inhibitor analysis suggested that the redox cycling of MitoQ occurred at two sites on complex I, proximal and distal to the rotenone-binding site. This was confirmed by demonstrating the redox cycling of MitoQ on purified mitochondrial complex I as well as NADH-fueled submitochondrial particles. Mitoquinone time- and dose-dependently increased endothelial cell apoptosis. These findings demonstrate that MitoQ may be prooxidant and proapoptotic because its quinone group can participate in redox cycling and superoxide production. In light of these results, studies using mitoquinone as an antioxidant should be interpreted with caution. *Antioxid. Redox Signal.* 9, 1825–1836.

INTRODUCTION

Reactive oxygen species (ROS) derived from mitochondria play a major role in promoting age-related human diseases, vascular and neurologic complications of diabetes, and cell damage in neurodegenerative disorders (10, 25, 30). Aberrant electron leakage from the mitochondrial respiratory chain is well known to reduce molecular oxygen to form superoxide ($O_2^{\bullet}$), contributing to oxidative mitochondrial damage (4). The ubiquinone derivative mitoquinone (MitoQ) is a novel drug thought to protect mitochondria from oxidative damage. Mitoquinone is targeted to mitochondria through its triphenylphosphonium cationic moiety that facilitates drug accumulation because of the large negative mitochondrial membrane potential (16). Mitoquinone protected against lipid peroxidation in rat liver mitochondria and prevented hydrogen peroxide (H_2O_2)-induced apoptosis in mammalian cells (17). In bovine aortic endothelial cells (BAECs), MitoQ reduced oxidative damage induced by glucose and glucose oxidase (5). Although, MitoQ has been previously suggested to decrease mitochondrial ROS production, O'Malley *et al.* (23) demonstrated that it may actually enhance $O_2^{\bullet}$ production in mitochondria fueled by the complex I substrates, glutamate and malate. Evidence also suggests that MitoQ decreases bioavailability of mitochondrial nitric oxide through generation of ROS (13). More recently, MitoQ in concentrations as low as 30 n*M* has been shown to upregulate the expression of inflammatory markers such as ICAM-1 in human pulmonary endothelial cells (22).

Free Radical in Medicine Core, Division of Cardiology, Emory University School of Medicine, Atlanta, Georgia.

To address this controversy, we studied the effects of MitoQ on endothelial and mitochondrial ROS production and elucidated the molecular mechanisms of MitoQ-induced endothelial dysfunction. Evidently, MitoQ contains a quinone group, well known to have redox-cycling properties similar to those of menadione and geldanamycin (7,20). Quinones react with flavin-containing reductases to form semiquinone radicals that can in turn reduce oxygen to form $O_2^{\bullet}$. In this study, we used electron spin resonance (ESR) and high-performance liquid chromatography (HPLC) to examine the redox cycling properties of MitoQ and study its effect on mitochondrial and cellular oxidative stress. Our findings demonstrate that concentrations of this drug commonly used in biologic studies produce large amounts of $O_2^{\bullet}$ both in cell-free systems and when exposed to isolated mitochondria or intact endothelial cells. Moreover, our data show that the redox cycling of MitoQ occurs at more than one site on complex I. These results raise concerns regarding the use of this agent as a mitochondria-targeted antioxidant and raise questions concerning its application as a therapeutic agent.

MATERIALS AND METHODS

Reagents

Mitoquinone (MitoQ) was a gift from Dr. Jay Joseph (Medical College of Wisconsin, Milwaukee, WI) and was dissolved in ethanol. Dihydroethidium was purchased from Molecular Probes (Eugene, OR). Horseradish peroxidase (HRP) and NADPH-P450 reductase were obtained from Calbiochem (San Diego, CA). 1-Hydroxy-2,2,6,6-tetramethylpiperidin-4-yl-trimethylammonium (CAT1H) and 2-ethoxycarbonyl-2-methyl-3,4-dihydro-2*H*-pyrrole-1-oxide (EMPO) were purchased from Alexis Corporation (San Diego, CA). All other reagents were obtained from Sigma (St. Louis, MO).

Measurements of ROS production in cell-free systems, isolated mitochondria, submitochondrial particles, and purified complex I were performed in media A buffer containing 125 m*M* KCl, 10 m*M* MOPS, 2 m*M* $MgSO_4$, 2 m*M* KH_2PO_4, 10 m*M* NaCl, 1 m*M* EGTA, and 0.7 m*M* $CaCl_2$, pH 7.2. This buffer was treated with 50 μM desferoxamine to chelate free iron. Determination of endothelial $O_2^{\bullet}$ production was carried out in Krebs-HEPES buffer containing 5.786 g/L NaCl, 0.35 g/L KCl, 0.368 g/L $CaCl_2$, 0.296 g/L $MgSO_4$, 2.1 g/L $NaHCO_3$, 0.142 g/L K_2HPO_4, 5.206 g/L Na-HEPES, 2 g/L D-glucose, pH 7.35.

Stock solutions of CAT1H (10 m*M*), dissolved in 0.9% NaCl treated with 50 g/L chelex 100 and containing 50 μM desferoxamine and purged with argon, were prepared daily and kept under argon on ice. Desferoxamine was used to decrease autooxidation of CAT1H catalyzed by trace amounts of free iron. CAT1H was used in a final concentration of 1 m*M*.

Cell culture and mitochondrial isolation

Bovine aortic endothelial cells (passage four to eight) (Cell Systems, Kirkland, WA) were cultured on 100-mm plates in Media 199 containing 10% fetal calf serum supplemented with 2 m*M* L-glutamine and 1% vitamins. On the day before the study, the fetal calf serum concentration was reduced to 1%. Confluent BAECs were used for the experiments. Endothelial cell mitochondria were isolated as previously described (26). In brief, the cells were incubated in the presence or absence of MitoQ (0.01–1 μM for 1 h), and then washed twice with the isolation buffer containing 225 m*M* mannitol, 75 m*M* sucrose, 20 m*M* MOPS, 1 m*M* EGTA, 0.1% BSA, pH 7.2, adjusted with Tris. The cells were harvested by scraping and centrifugation with a low-speed spin at 937 *g* for 5 min. The pelleted cells were incubated for 5–10 min in a low-tonicity 100-mOsm medium containing 100 m*M* sucrose, 10 m*M* MOPS, 1 m*M* EGTA, 0.1% BSA, pH 7.2, and disrupted by 25–30 sharp strokes of the tight pestle in a Dounce homogenizer. The medium's tonicity was adjusted to 300 mOsm with 1.25 *M* sucrose, and the volume tripled with the isolation buffer. The disrupted cells were centrifuged for 5 min at 1,075 *g*. The supernatant was spun at 9,300 *g* for 10 min. The supernatant was removed and used for the cytoplasmic fraction assay to assess the purity of our mitochondrial preparation. The remaining sediment was resuspended in isolation medium and centrifuged at 1,075 *g* for 5 min. The final supernatant was centrifuged at 8,600 *g* for 10 min. The last sediment was resuspended in 0.25 *M* sucrose, 10 m*M* MOPS, and 1 m*M* EGTA, at pH 7.2.

Purity of mitochondria

To assess the purity of our mitochondrial fractions, mitochondrial and cytoplasmic fractions prepared from BAECs, as mentioned earlier, were subjected to Western blot analysis. Mouse monoclonal antibodies (Santa Cruz Biotechnology, Inc., Santa Cruz, CA) directed toward glyceraldehyde 3-phosphate dehydrogenase (GAPDH) and cytochrome oxidase (COX) subunit I were used to verify the integrity of these subcellular fractions.

Preparation of the submitochondrial particles

The inverted nonphosphorylating submitochondrial particles (SMPs) were prepared according to Panov *et al*. (25). Fresh endothelial mitochondria were suspended in 0.25 *M* sucrose with 2 m*M* EDTA. The suspension was saturated with N_2, placed into a beaker filled with a mixture of ice and water for effective cooling, and subjected to sonic oscillations (5 times for 5 sec). The sonicated mitochondria were diluted with a double volume of 0.25 m*M* sucrose buffered with 10 m*M* MOPS, and centrifuged in a Beckman ultracentrifuge at 16,000 *g* for 10 min. The supernatant was centrifuged at 150,000 *g* for 45 min. The sediment of SMPs was collected and homogenized in a small glass homogenizer in a volume of 0.25 *M* sucrose.

Isolation of mitochondrial complex I (NADH-ubiquinone oxidoreductase)

Mitochondrial complex I isolation was carried out as previously described (15). In brief, mitochondria (2 mg) were diluted in 200 μl buffer containing 50 m*M* Tris-HCl, 1 μg/ml pepstatin, 1 μg/ml leupeptin, 1 m*M* phenyl-methylsulfonyl flu-

oride (PMSF), and 1% *n*-dodecyl-β-D-maltoside (LM). The mixture was incubated on ice for 30 min and then centrifuged for 10 min at 72,000 *g*. The resultant supernatant was incubated overnight with 10 μl capture resin MS101 (MitoSciences, Inc., Eugene, OR) containing the anti-complex I immunocapture monoclonal antibody covalently linked to protein G agarose beads. Beads were collected by gentle centrifugation (10 sec at 500 *g*) and washed twice for 5 min in PBS and 0.05% LM. Complex I was eluted from the resin by addition of 50 μl 1% SDS. All preparations were always performed at 4°C.

Measurement of $O_2^{\bullet}$ production

Superoxide production was analyzed in cytochrome P-450 reductase system by two different methods: (a) spin trapping of $O_2^{\bullet}$ with EMPO, and (b) using ESR with the cell-impermeable spin probe CAT1H. CAT1H reacts with $O_2^{\bullet}$ radicals to form a stable nitroxide radical (Fig. 1, reaction 1). Superoxide production was determined by SOD-inhibitable oxidation of CAT1H with 50 U/ml Cu,Zn-SOD. We have previously validated our ESR assay by using CAT1H in xanthine plus xanthine oxidase cell-free system, as illustrated in Fig. 1A. Superoxide generation by complex I and SMP was determined by using ESR and the spin-trap EMPO.

Measurements of intracellular $O_2^{\bullet}$ production

Intracellular $O_2^{\bullet}$ generation by BAECs was quantified by using dihydroethidium and an HPLC-based assay, as described previously (9). In brief, the cells were rinsed twice with chilled Krebs-HEPES buffer and then exposed to 10 μ*M* dihydroethidium for 20 min at 37°C in Krebs-HEPES buffer. The cells were then harvested by scraping and were placed in 300 μl of cold methanol, homogenized, and filtered (0.22 μm). Separation of ethidium and 2-hydroxyethidium was performed by using a Beckman HPLC System Gold model with a C-18 reverse-phase column (Nucleosil 250; 4.5 mm; Sigma-Aldrich), equipped with a fluorescence detector. Fluorescence detection at 580 nm (emission) and 480 nm (excitation) was used to monitor 2-hydroxyethidium production. The mobile phase was composed of a gradient containing 60% acetonitrile and 0.1% trifluoroacetic acid. Ethidium and 2-hydroxyethidium were separated by a linear increase in acetonitrile concentration from 37 to 47% over 23 min at a flow rate of 0.5 ml/min.

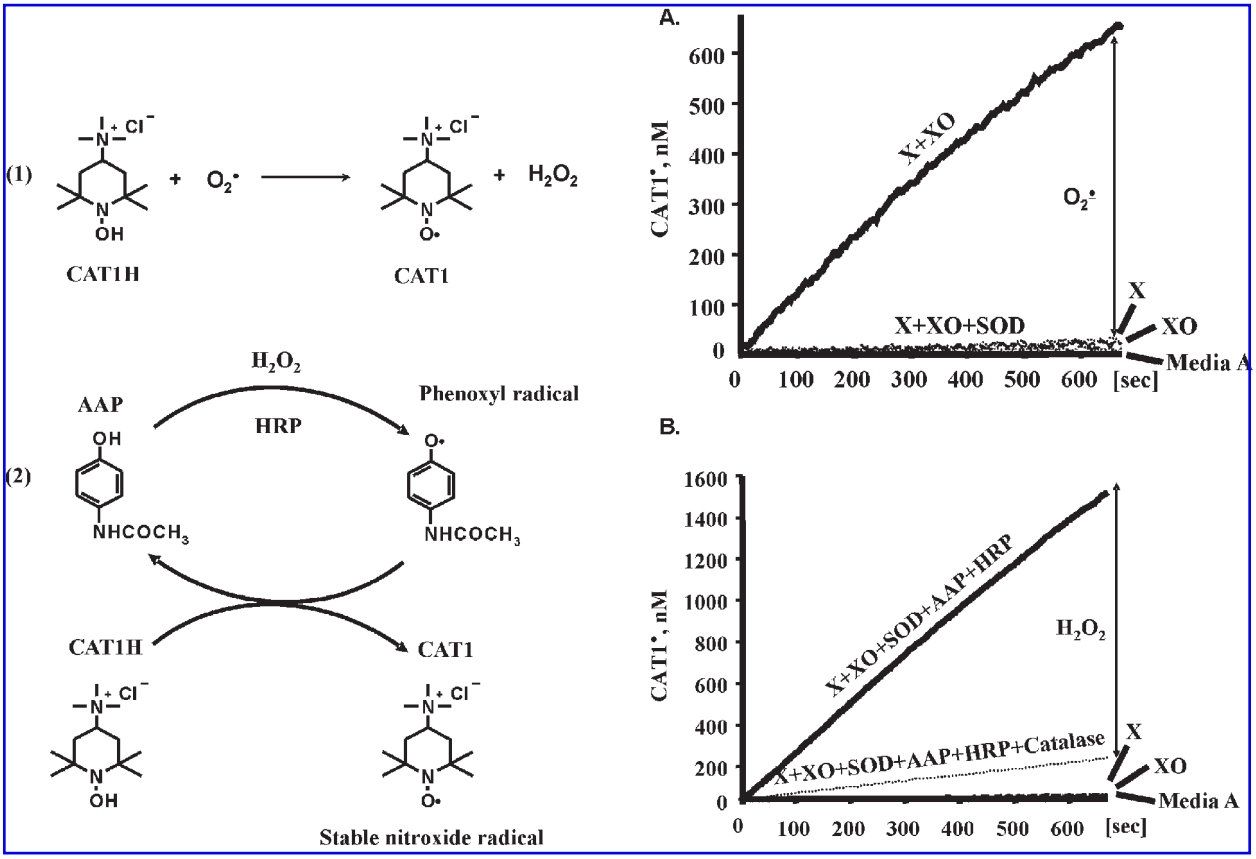

FIG. 1. Measurement of $O_2^{\bullet}$ and H_2O_2 release by using ESR and the spin-probe CAT1H. (**A**) Quantification of $O_2^{\bullet}$ radical in xanthine (X) plus xanthine oxidase (XO, 0.5 mU/ml) cell-free system. SOD-inhibited CAT1-nitroxide formation reflects the amount of $O_2^{\bullet}$ detected by CAT1H. (**B**) Production of H_2O_2 was measured by co-oxidation of CAT1H in horseradish peroxidase (HRP)–acetamidophenol (AAP) reaction, as described in Methods (reaction 2). Detection of H_2O_2 was verified by inhibition with 50 μg/ml catalase in a cell-free system containing xanthine (X) and xanthine oxidase (XO).

Measurement of mitochondrial ROS production

Mitochondrial ROS production was determined by mixing 20 μg of mitochondrial protein in media A with 1 m*M* 4-acetamidophenol (AAP), 5 U/ml HRP, 50 U/ml Cu/Zn-superoxide dismutase (SOD), and 1 m*M* CAT1H (18). This method takes advantage of the formation of an HRP compound I, which in turn oxidizes AAP. Subsequently, AAP radical oxidizes CAT1H to its corresponding nitroxide radical (Fig. 1, reaction 2). Detection of H_2O_2 was confirmed by inhibiting the ESR signal with 50 μg/ml catalase in xanthine plus xanthine oxidase cell-free system (Fig. 1B).

ESR experiments

All ESR samples were prepared using media A, pH 7.2, and were placed in 50-μl glass capillaries (Corning, New York, NY). To inhibit iron-catalyzed reactions, desferoxamine (50 μM) was added to all samples. ESR spectra were recorded by using an EMX ESR spectrometer (Bruker Biospin Corp., Billerica, MA) and a super high Q microwave cavity at room temperature. The ESR settings for field-scan experiments with the spin-trap EMPO or the spin probe CAT1H were as follows: field sweep, 70 gauss; microwave frequency, 9.82 GHz; microwave power, 20 mW; modulation amplitude, 0.7 gauss; conversion time, 41 msec; time constant, 164 msec; and receiver gain, 1×10^5 ($n = 4$ scans). ESR spin-trapping experiments were done at least 3 times.

The kinetics of ROS production was recorded by monitoring the amplitude of the low field component of the ESR spectrum of CAT1-nitroxide with the following settings: field sweep, 60 gauss; microwave frequency, 9.46 GHz; microwave power, 20 mW; modulation amplitude, 2 gauss; conversion time, 1,311 msec; time constant, 5,243 msec; and receiver gain, 1×10^5.

Caspase-3 activity assay

Caspase-3 activity was measured after the exposure of endothelial cells to MitoQ (0.1 or 1 μM) for 1–4 h by using Western blot analysis. In brief, endothelial cells were rinsed twice in ice-cold PBS and lysed in lysis buffer containing 1% nonylphenol polyoxyethylene 40 (NP-40), 100 m*M* Na_3VO_4, 5 m*M* EGTA, 10 m*M* $Na_4P_2O_7$, 100 m*M* phenyl-methylsulfonyl fluoride (PMSF), and 2 μg/ml each of leupeptin, pepstatin, and aprotinin. Samples were centrifuged (10,000 *g*, 10 min), and the supernatant was retained for determination of caspase-3 activity and protein concentration. The protein concentration in the supernatant was determined by using the Bradford Assay. Equal amounts of protein samples (50 μg) were separated in 12% SDS-PAGE. Polyclonal anti-caspase (1:1,000) antibody (Cell Signaling, Danvers, MA) were used to detect the endogenous levels of the large fragment (17 kDa) resulting from proteolytic processing of the inactive full-length caspase-3 into activated p17 and p12 fragments. The densitometry of the cleaved caspase-3 and α-actin bands was performed with a Gel Doc 1000 system (Bio-Rad Laboratories).

Data analysis

All data are expressed as mean ± SEM. Comparisons between groups of treatments were made by one-way ANOVA, followed by Bonferroni–Dunn *post hoc* test when significance was indicated. Values of $p < 0.05$ were considered significant.

RESULTS

Mitoquinone promotes $O_2^{\bullet-}$ production from purified NADPH cytochrome P-450 reductase

Previously, it was found that quinone-containing compounds undergo one-electron reductions by flavin-containing enzymes to form semiquinone radicals, which in turn may rapidly react with oxygen to generate $O_2^{\bullet-}$ (7). NADPH cytochrome P-450 reductase was used to determine whether MitoQ can redox cycle on flavin-containing enzymes. The ESR spectra of EMPO and CAT1H exposed to only MitoQ or NADPH and cytochrome P-450 showed no detectable signal. The addition of NADPH cytochrome P-450 reductase to the sample containing MitoQ and NADPH caused the formation of a strong ESR signal with both EMPO and CAT1H, which was inhibited by Cu/Zn-SOD, confirming redox cycling of MitoQ (Fig. 2A). Mitoquinone increased $O_2^{\bullet-}$ production in a concentration-dependent manner, and the intensity of the ESR spectra was significantly higher compared with that of equivalent concentrations of menadione, convincingly demonstrating that MitoQ is markedly efficient in redox cycling (Fig. 2B). The ESR spectrum of MitoQ after exposure to the NADPH cytochrome P-450 reductase without the spin-trap EMPO or the spin-probe CAT1H revealed a weak but detectable ESR signal compatible with a semiquinone of MitoQ. These results demonstrate a one-electron reduction of MitoQ by the NADPH cytochrome P-450 reductase (Fig. 2C), which leads to redox cycling of MitoQ and $O_2^{\bullet-}$ production.

Stimulation of $O_2^{\bullet-}$ production in endothelial cells by mitoquinone

As noted earlier, MitoQ redox cycles on flavin-containing enzymes and produces $O_2^{\bullet-}$ in cell-free systems. We therefore sought to determine the effect of MitoQ on intracellular $O_2^{\bullet-}$ production in BAECs. Endothelial cells were exposed to increasing concentrations of MitoQ (1, 5, 10, 100, and 1,000 n*M*) for 1 h and then analyzed by using HPLC and dihydroethidium. Mitoquinone dose-dependently increased intracellular $O_2^{\bullet-}$ production (Fig. 3). These results clearly indicate that MitoQ in concentrations commonly applied in biologic studies markedly increases intracellular $O_2^{\bullet-}$ production in BAECs.

Stimulation of H_2O_2 production in isolated mitochondria by mitoquinone

These data strongly suggest that MitoQ is an *in vivo* prooxidant that produces ROS in intact endothelial cells. A probable mechanism by which MitoQ triggers intracellular ROS production is through its redox cycling in mitochondria, in which its ubiquinone moiety inserts into the lipid bilayer (16). In the first series of experiments, the ability of MitoQ to induce ROS generation in mitochondria isolated from endothelial cells was studied. Because the mitochondrial inner-membrane is not permeable to $O_2^{\bullet-}$, and intramitochondrial manganese SOD readily

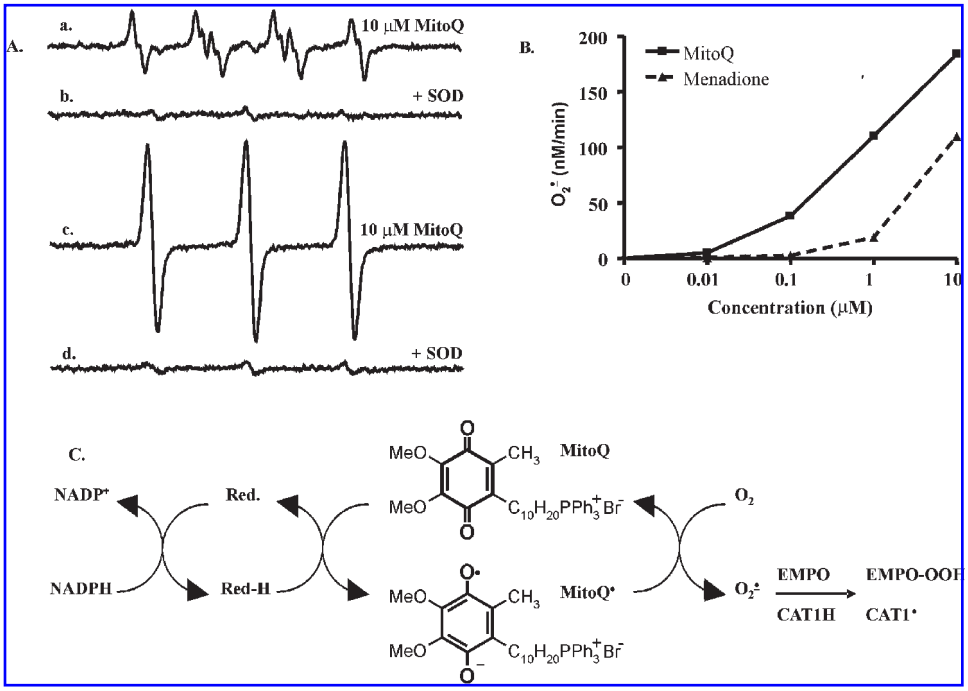

FIG. 2. (A) ESR detection of $O_2^{\bullet}$ production by MitoQ with NADPH cytochrome P-450 reductase using EMPO or CAT1H. (a) ESR spectra of sample containing spin-trap EMPO (50 m*M*), NADPH (0.3 m*M*), cytochrome P-450 reductase (5 μg/ml), and MitoQ (10 μM). (b) Same as (*a*) plus 50 units/ml Cu/Zn-SOD. (c) ESR spectra of sample containing cytochrome P-450 reductase (5 μg/ml), CAT1H (1 m*M*), NADPH (0.3 m*M*), and MitoQ (10 μM). (d) Same as (c) plus 50 units/ml Cu/Zn-SOD. (**B**) Rate of $O_2^{\bullet}$ production by MitoQ *vs*. menadione with NADPH cytochrome P-450 reductase determined by using ESR and the spin-probe CAT1H. Conditions are similar to those in (**A**). Data are expressed as means ($n = 3$ experiments). (**C**) Reaction equation for the redox cycling of MitoQ.

converts $O_2^{\bullet}$ into H_2O_2, which is diffusible across the mitochondrial membranes (3), ROS production from intact mitochondria was determined from the amount of H_2O_2 released.

Intact mitochondria were isolated from BAECs and acutely treated with MitoQ (0.01–10 μM). The purity of our mitochondrial fractions was substantiated by detecting the cytoplasmic marker GAPDH exclusively in the cytoplasmic but not in the mitochondrial fraction, whereas the COX subunit I was detected preferentially in the mitochondrial but not in the cytoplasmic fraction (Fig. 4A). Extramitochondrial H_2O_2 pro-

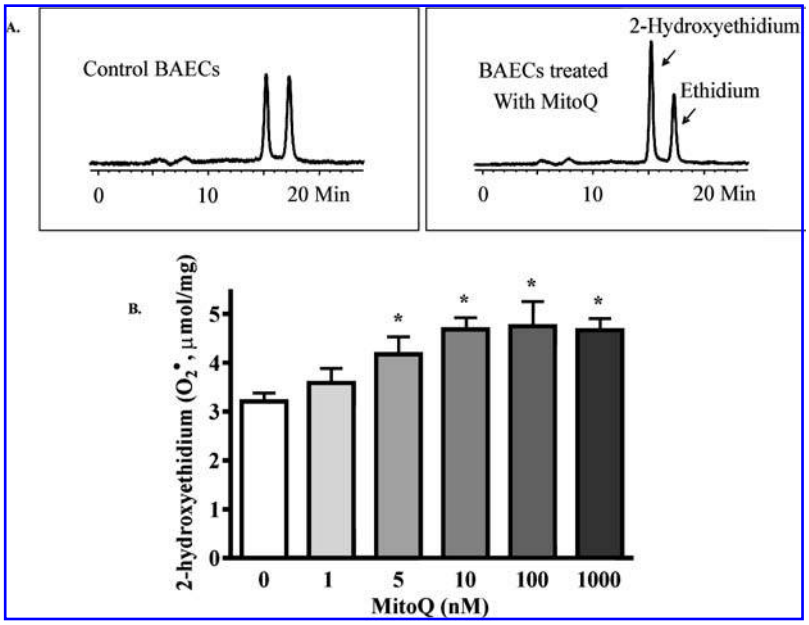

FIG. 3. High-performance liquid chromatography/dihydroethidium detection of MitoQ-induced endothelial $O_2^{\bullet}$ production. (**A**) High-performance liquid chromatograms of ethidium and 2-hydroxyethidium formed by exposure of dihydroethidium to intracellular $O_2^{\bullet}$. Formation of 2-hydroxyethidium is proportional to the rate of $O_2^{\bullet}$ production (9). (**B**) Bovine aortic endothelial cells were incubated with MitoQ (10–1,000 n*M*) for 1 h at 37°C. Superoxide production was determined by the formation of 2-hydroxyethidium. Fluorescence detection at 580 nm (emission) and 480 nm (excitation) was used to monitor 2-hydroxyethidium production. Data are expressed as mean ± SEM ($n = 5$ experiments). *$p < 0.05$ *vs*. control.

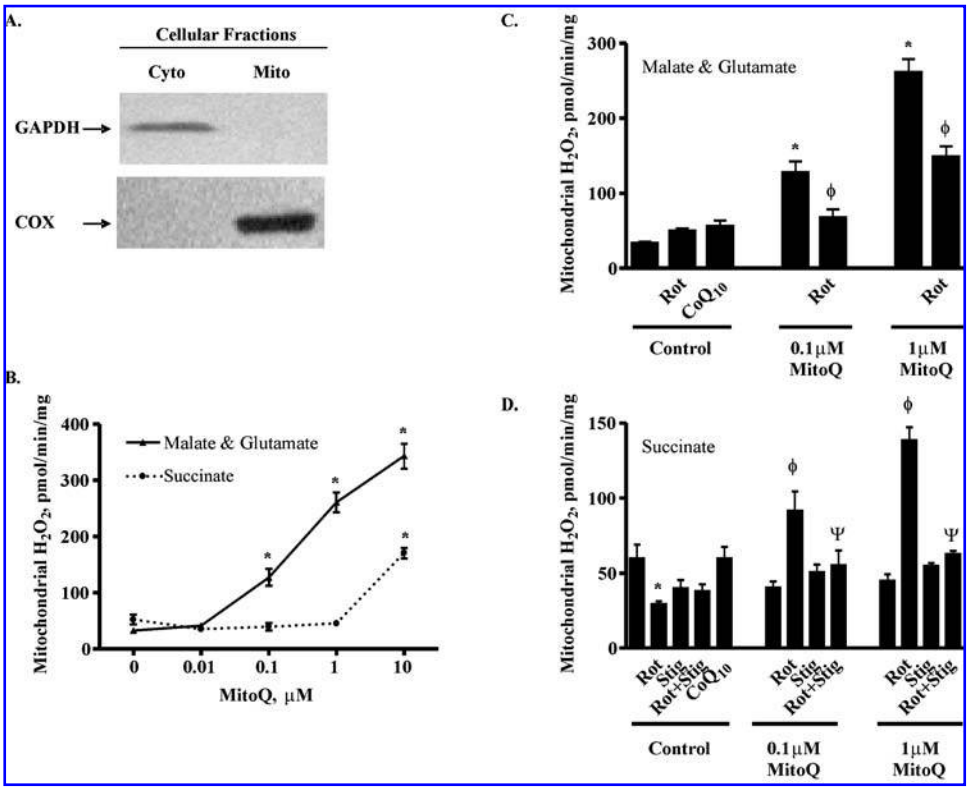

FIG. 4. Hydrogen peroxide production (mean ± SEM) quantified by ESR in isolated BAECs mitochondria treated acutely with MitoQ. (**A**) Western blot analysis of mitochondrial (mito) and cytoplasmic (cyto) fractions that were probed with antibody directed toward GAPDH and COX subunit I. (**B**) Rate of H_2O_2 production in isolated BAECs mitochondria fueled with 2 m*M* malate and 20 m*M* glutamate or 5 m*M* succinate in the presence of mitoquinone (MitoQ, 0.01–10 μM). (**C**) Hydrogen peroxide production in isolated BAECs mitochondria fueled with 2 m*M* malate and 20 m*M* glutamate in the presence of 0.1 or 1 μM MitoQ or 10 μM ubiquinone (CoQ_{10}). (**D**) Hydrogen peroxide production in isolated BAECs mitochondria fueled with 5 m*M* succinate in the presence of 0.1 or 1 μM MitoQ or 10 μM ubiquinone (CoQ_{10}). For each group along the x axis, mitochondria were exposed to 5 μM rotenone (Rot), or 80 n*M* stigmatellin (Stig) or both. $^*p < 0.01$ compared with control; $\phi p < 0.05$ compared with mitochondria treated with MitoQ in the absence of rotenone; $\Psi p < 0.05$ compared with mitochondria treated with MitoQ in the presence of rotenone ($n = 4$ for each condition).

duction was measured by using the HRP-AAP–coupled co-oxidation of the cyclic hydroxylamine CAT1H (18). Hydrogen peroxide production was markedly increased in glutamate plus malate–fueled mitochondria as a function of MitoQ concentrations (Fig. 4B). Unlike malate plus glutamate, H_2O_2 production by mitochondria fueled with succinate increased only with 10 μM MitoQ. Interestingly, MitoQ (0.01–1 μM) had mild inhibitory effects on H_2O_2 production in succinate-fueled mitochondria. These results are consistent with data previously published by O'Malley *et al.* (23), suggesting that MitoQ increases mitochondrial ROS production.

To determine the potential site of MitoQ redox cycling in malate plus glutamate–fueled mitochondria, we examined the effect of rotenone on ROS generation triggered by MitoQ. Rotenone inhibits the transfer of electrons from the reduced iron-sulfur cluster (N2) to bound ubiquinones in complex I (24). Addition of rotenone to control mitochondria in the presence of complex I substrates mildly increased ROS generation. In contrast, rotenone partially but significantly inhibited the MitoQ-mediated H_2O_2 production in the presence of complex I substrates (Fig. 4C). The rotenone effect in malate plus glutamate–fueled mitochondria was compared with that in the presence of the complex II substrate, succinate. In this case, rotenone decreased H_2O_2 production in control mitochondria. In mitochondria treated with MitoQ, rotenone significantly enhanced succinate-driven H_2O_2 production (Fig. 4D). The effect of rotenone to decrease H_2O_2 production in forward electron transfer suggests that the site of MitoQ redox cycling is proximal to complex II and most likely on complex I. Redox cycling of MitoQ at the level of complex I is also evidenced by the fact that stigmatellin, an inhibitor of electron transport at Q_o center of complex III, prevented rotenone-induced increase in ROS production by mitochondria treated with MitoQ and fueled with succinate (Fig. 4D). Stigmatellin inhibits reverse electron transport from complex II to complex I *via* dissipation of the mitochondrial membrane potential (21). In untreated mitochondria, stigmatellin decreased the level of succinate-driven ROS production. Interestingly, the addition of 10 μM native ubiquinone-10 (CoQ_{10}) to isolated mitochondria did not have any effect on mitochondrial ROS production with both complex I and II substrates (Fig. 4C and D).

It is noteworthy that the addition of ethanol, which was used

as a solvent for MitoQ, rotenone, and stigmatellin, had no effect on mitochondrial ROS production (data not shown).

Effect of mitoquinone treatment of intact BAECs on mitochondrial ROS production

In the second series of experiments, we evaluated whether similar effects will be observed in mitochondria isolated after prior exposure of intact endothelial cells to MitoQ. Cells were treated with MitoQ (0.01–1 μM) for 1 h before isolation of mitochondria. Analysis showed similar effects to those observed when MitoQ was added after mitochondrial isolation. Preincubation of endothelial cells with MitoQ caused a concentration-dependent increase in the rate of mitochondrial H_2O_2 production with complex I substrates. Mitoquinone did not have any effects on H_2O_2 production in succinate-fueled mitochondria (Fig. 5A). Next we determined the effect of rotenone and stigmatellin on the rate of mitochondrial ROS production. Rotenone significantly inhibited MitoQ-induced H_2O_2 generation in glutamate plus malate–fueled mitochondria (Fig. 5B). In contrast, treatment with rotenone markedly enhanced succinate-driven H_2O_2 production (Fig. 5C). These effects were similar to those observed for intact mitochondria treated acutely with MitoQ. We also found that the combination of rotenone and stigmatellin had similar effects on succinate-driven mitochondrial H_2O_2 production to those observed with acutely treated mitochondria. These findings argue that MitoQ is accumulated in mitochondria where redox cycling and ROS generation occur at the level of complex I.

Mitoquinone promotes $O_2^{\bullet-}$ Production from SMP and purified mitochondrial complex I

As noted earlier, MitoQ stimulated H_2O_2 production in endothelial mitochondria. Inhibitor analysis with rotenone or stigmatellin or both suggested that MitoQ-derived ROS occurs primarily on complex I. To confirm this, we sought to determine directly whether MitoQ can redox cycle on purified mitochondrial complex I. As seen in Fig. 6, MitoQ dose-dependently increased $O_2^{\bullet-}$ production from SMP (see Fig. 6A and D) and isolated complex I (Fig. 6B and D) in the presence of NADH.

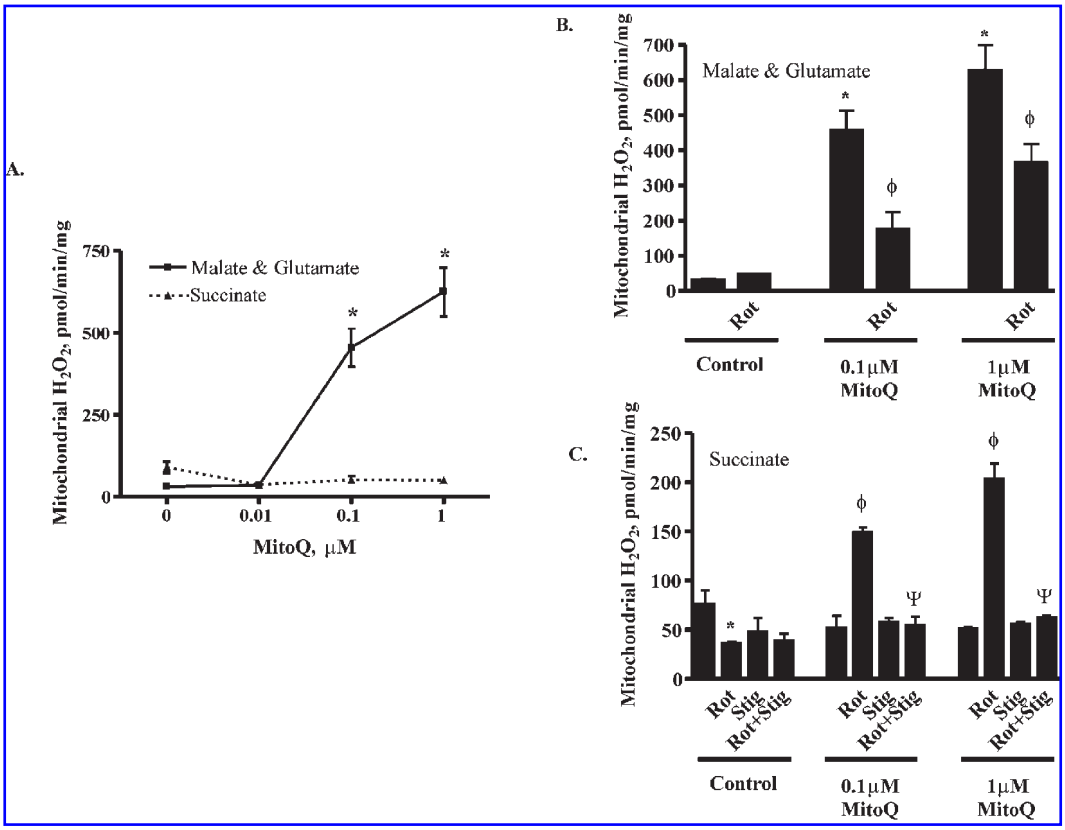

FIG. 5. Hydrogen peroxide production (mean ± SEM) quantified by ESR in mitochondria isolated from BAECs pretreated with MitoQ for 1 h. (**A**) Rate of H_2O_2 production in intact mitochondria isolated after 1-h exposure of BAECs to MitoQ (MitoQ, 0.01–10 μM) fueled with 2 mM malate and 20 mM glutamate or 5 mM succinate. (**B**) Hydrogen peroxide production in isolated BAECs mitochondria fueled with 2 mM malate and 20 mM glutamate. (**C**) Hydrogen peroxide production in isolated BAECs mitochondria fueled with 5 mM succinate. For each group along the x axis, mitochondria were exposed to 5 μM rotenone (Rot), or 80 nM stigmatellin (Stig), or both. *$p < 0.01$ compared with control; $\phi p < 0.05$ compared with mitochondria isolated from BAECs treated with MitoQ; $\Psi p < 0.05$ compared with mitochondria isolated from BAECs treated with MitoQ in the presence of rotenone. Values represent the means of at least three experiments.

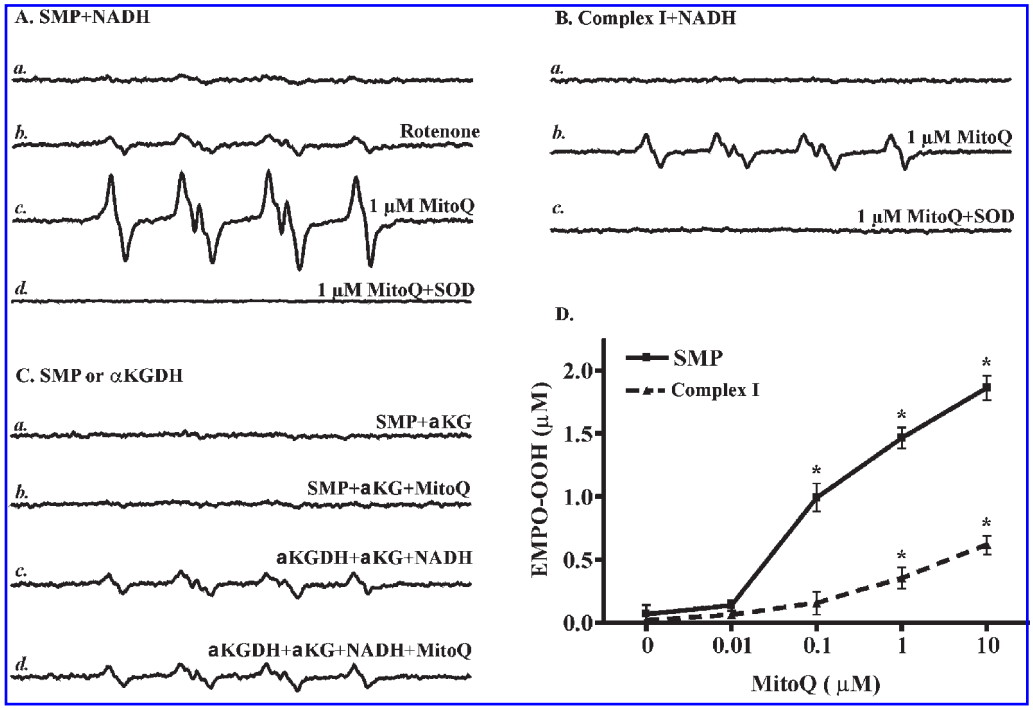

FIG. 6. ESR detection of $O_2^{\bullet}$ production by MitoQ with (A) submitochondrial particles (SMP), (B) isolated complex I, and (C) purified α-ketoglutarate dehydrogenase complex using EMPO. (**A**) *a*, ESR spectrum of sample containing spin-trap EMPO (50 m*M*), NADH (40 μM), and SMP (0.2 mg/ml); *b*, same as *a* plus rotenone (5 μM); *c*, same as *a* plus MitoQ (1 μM); *d*, same as *c* plus 50 units/ml Cu/Zn-SOD. (**B**) *a*, ESR spectrum of sample obtained by mixing 50 m*M* EMPO, 40 μM NADH, and complex I (0.1 mg/ml); *b*, same as *a* plus 1 μM MitoQ; *c*, same as *b* plus 50 units/ml Cu/Zn-SOD. (**C**) *a*, ESR spectrum of sample obtained by mixing 50 m*M* EMPO, 0.2 mg/ml SMP, and 1 m*M* α-ketoglutarate (αKG); *b*, same as *a* plus 1 μM MitoQ; *c*, ESR spectrum of sample containing 50 m*M* EMPO, 40 μM NADH, 1 m*M* αKG, and 20 μg α-ketoglutarate dehydrogenase (αKGDH); *d*, same as *c* plus 1 μM MitoQ. (**D**) Rate of $O_2^{\bullet}$ production in SMP and isolated complex I after acute treatment with MitoQ (0.01–10 μM). *$p < 0.05$ compared with control. Values represent the means of at least three experiments.

Recent evidence suggests that the α-ketoglutarate dehydrogenase complex (αKGDH), an integral TCA-cycle enzyme tightly bound to the inner mitochondrial membrane on the matrix side mediates ROS production in mitochondria fueled with malate and glutamate or α-ketoglutarate (αKG) (11, 29). We tested whether αKGDH could account for the increase in ROS production in the presence of MitoQ. Mitoquinone did not affect ROS production by SMP fueled with αKG, nor did it increase the level of $O_2^{\bullet}$ produced by purified αKGDH in the presence of NADH and αKG (see Fig. 6C). This result argues against a role for αKGDH in redox cycling of MitoQ.

Mitoquinone stimulates apoptosis in BAECs

Bovine aortic endothelial cells were incubated with MitoQ (0.1 and 1 μM) for different time periods (1–4 h), and the caspase-3 activities were measured as a function of time. The caspase-3 activity was markedly elevated after 3- and 4-h incubation with 1 μM MitoQ. Figure 7A and B shows that 0.1 μM Mito-Q also increased the activity of caspase-3; however, this increase was only significant after 4-h incubation. In line with the fact that mitochondrial oxidative damage may result in cellular apoptosis, MitoQ at a concentration of 0.1 and 1 μM time dependently stimulates endothelial cell apoptosis (Fig. 7).

DISCUSSION

These experiments demonstrate that MitoQ, in concentrations commonly used in biologic studies, redox cycles and yields $O_2^{\bullet}$ radicals on exposure to flavin-containing enzymes. In addition, MitoQ at low concentrations markedly increased endothelial $O_2^{\bullet}$ production and complex I–driven mitochondrial H_2O_2 production. Our studies also indicate that this effect of MitoQ time-dependently stimulates the activity of caspase-3, resulting in endothelial cell apoptosis.

In 2001, Murphy and co-workers (16) reported the development of a novel antioxidant targeted to mitochondria by covalent attachment of a quinone group to a lipophilic triphenylphosphonium cation, named MitoQ, which may selectively block mitochondrial oxidative damage. Based on these findings, other groups showed that MitoQ applied at concentrations ranging from 10 n*M* to 10 μM suppressed ROS production and protected against apoptosis in cells exposed to H_2O_2 or glucose and glucose oxidase (5, 8, 16, 28). The assumption has been made that MitoQ is an effective mitochondrial antioxidant until recently, when O'Malley et al. (23) demonstrated that MitoQ increases ROS production in glutamate plus malate–fueled mitochondria. Similarly, MitoQ (30–100 n*M*) has been shown to create a stressful situation in human pulmonary endothelial

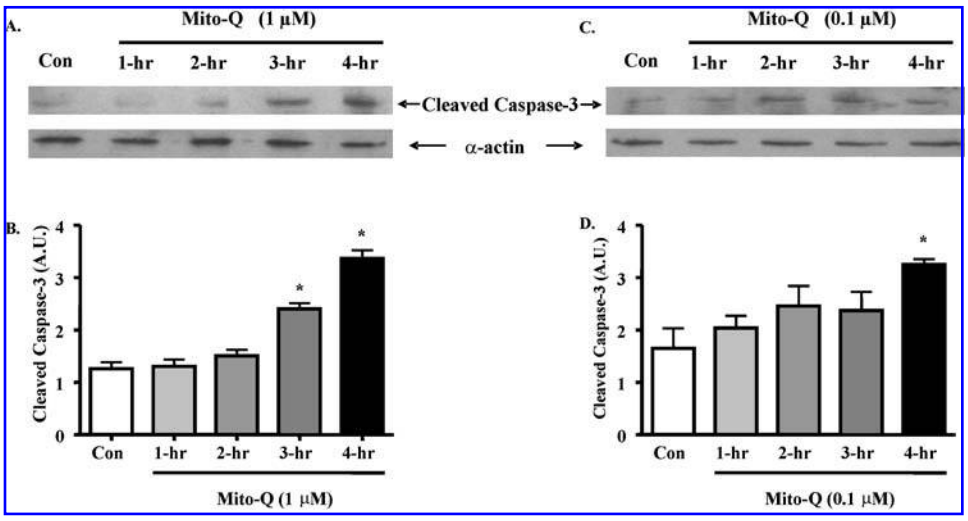

FIG. 7. Caspase-3 activity in mitoquinone-treated endothelial cells. Caspase-3 activity was measured as an indicator of apoptotic cell death by using Western blot analysis after 1-, 2-, 3-, and 4-h exposure of cultured endothelial cells to 0.1 or 1 μM MitoQ. The results were expressed as arbitrary units. The top panels are representative Western blots, and the bottom panels are grouped densitometric data presented as mean ± SEM. $n = 4$ experiments for each condition, $^*p < 0.05$ *vs*. control.

cells, resulting in the generation of ROS, enhanced NF-κB activation, and upregulation of ICAM-1 expression (22). Although the mechanism of such an increase in ROS production was not defined in these previous studies, their results did suggest that MitoQ possesses redox active properties and is therefore able to act as a prooxidant. Our current findings provide further details on the prooxidant activity of MitoQ. We demonstrated that MitoQ has redox-cycling property similar to menadione and geldanamycin and demonstrate that this cycling takes place at the level of complex I (7, 20).

Our results show that MitoQ increases mitochondrial H_2O_2 production in the presence of complex I substrates. This increase is significantly attenuated by the complex I inhibitor rotenone. Under normal conditions, NADH delivers electrons to the flavin (FMN) group, which routes these electrons to the iron-sulfur clusters and ultimately reduces the bound ubiquinone (UQ) group on complex I (Fig. 8). Rotenone is known to block electron transfer from the N2 iron-sulfur cluster to UQ (24). Therefore, in the presence of rotenone, only the proximal flavin group is reduced, as electrons cannot pass to the distal UQ group. The partial inhibition of the ESR signal with rotenone in the presence of complex I substrates implies that MitoQ is redox cycling at two sites. The first site is proximal to the rotenone-binding site on complex I, whereas the second is distal. Recent studies suggest that the reduced flavin group on complex I is a potential electron donor capable of electron redistribution to oxygen or other molecules. Interestingly, it is in a hydrophilic domain on the matrix side; therefore, it is easily accessible to the large hydrophilic core of MitoQ, whereas the FeS clusters are buried beneath the solvent-accessible surface (19, 27). This suggests that MitoQ most likely redox cycles at the flavin site on complex I (Fig. 8). Supporting this, MitoQ significantly enhanced $O_2^{\bullet}$ production from the purified flavin-containing enzyme cytochrome P-450 reductase in a cell-free system.

Conversely, the same effect was not observed with succinate. In mitochondria fueled with the complex II substrate, MitoQ alone did not increase or decrease mitochondrial ROS produc-

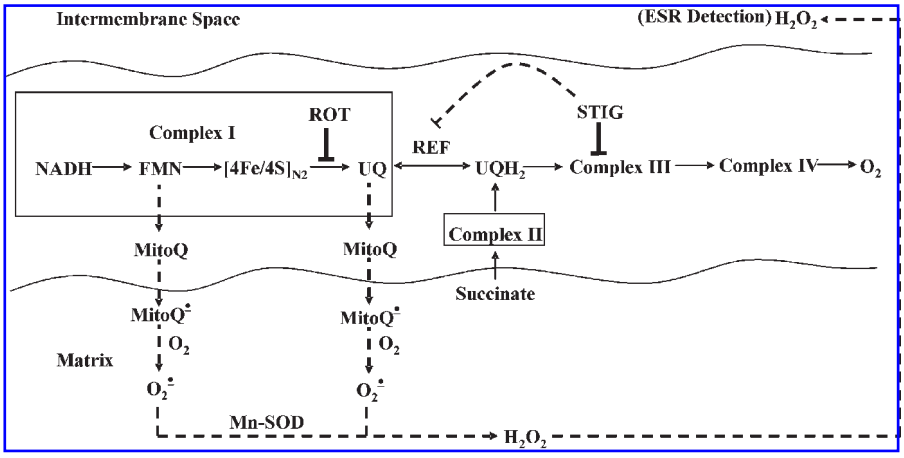

FIG. 8. Schematic diagram depicting electron transport, the action of substrates and inhibitors, and proposed sites of mitoquinone (MitoQ) redox cycling in endothelial cell mitochondria. *Straight lines with arrows*, Electron transport; *dashed lines*, redox cycling of MitoQ and $O_2^{\bullet}$ release or conversion to H_2O_2. Rotenone (ROT), stigmatellin (STIG), and reverse electron flow (REF).

tion, arguing against the hypothesis that MitoQ stops reverse electron flow from complex II to complex I (23). Interestingly, the addition of rotenone to succinate-fueled mitochondria resulted in a substantial and significant increase in ROS production in the presence of MitoQ (Figs. 4 and 5). This effect contrasts with that observed in control mitochondria where succinate-fueled ROS production is normally inhibited by rotenone (12). These results imply that by blocking reverse electron flow from the bound UQ group to the N2 iron-sulfur cluster on complex I with rotenone, the UQ group is overreduced, thus generating more semiquinone ($MitoQ^{\bullet}$) and $O_2^{\bullet}$ radicals (Fig. 8). Our theory of enhanced overreduction of the UQ site in the presence of rotenone is further emphasized by the finding that stigmatellin, a complex III inhibitor, abolished the effect of rotenone on succinate-derived ROS production in the presence of MitoQ. By inhibiting electron transport from the lipid-soluble ubiquinol (QH_2) to complex III, stigmatellin results in loss of the mitochondrial membrane potential on which reverse electron transport is dependent (21). This work shows that MitoQ redox cycles at a site distal to the rotenone-binding site, most likely at the level of the bound UQ group (Fig. 8).

Previously it was shown that the Krebs-cycle enzyme αKGDH is able to generate ROS (1, 11). Our current findings are in agreement with this observation. We found clear-cut evidence of $O_2^{\bullet}$ production by purified αKGDH in the presence of αKG and NADH; however, MitoQ failed to stimulate $O_2^{\bullet}$ production by αKGDH. Moreover, treatment of αKG-fueled SMP with MitoQ failed to show an increase in $O_2^{\bullet}$ generation. In contrast, MitoQ did increase $O_2^{\bullet}$ production in SMP and isolated complex I fueled with NADH. Furthermore, rotenone significantly decreased ROS production in the presence of MitoQ in intact mitochondria fueled with malate and glutamate. These data clearly demonstrate that MitoQ redox cycles on complex I and argue against a role for the Krebs-cycle enzyme αKGDH.

Therefore, we propose the following reactions scheme. MitoQ is reduced to a semiquinone radical ($MitoQ^{\bullet}$) at the level of complex I (reaction 1). This reaction may occur through potentially one of two mechanisms: the first one is transfer of electrons from the reduced flavin group to MitoQ, and the second one is reduction of MitoQ at the level of the bound UQ group (Fig. 8)

$$MitoQ + e^{-} \rightarrow MitoQ^{\bullet} \quad (1)$$

The radical thus generated reacts rapidly with oxygen to form $O_2^{\bullet}$ radicals (reaction 2), in equilibrium with its protonated form, hydroxyperoxyl radical ($HOO^{\bullet}$) (reaction 3).

$$MitoQ^{\bullet} + O_2 \rightarrow MitoQ + O_2^{\bullet} \quad (2)$$

$$O_2^{\bullet} + H_2O \leftrightarrow HO_2^{\bullet} + OH^{-} \quad (3)$$

The $O_2^{\bullet}$ anion reacts with the hydroxyperoxyl radical to form H_2O_2 and molecular oxygen (reaction 4). Alternatively, SOD can catalyze the dismutation of two $O_2^{\bullet}$ radicals to give one molecule of H_2O_2 and one of oxygen (reaction 5).

$$HO_2 + O_2^{\bullet} \rightarrow H_2O_2 + O_2 \quad (4)$$

$$2\ O_2^{\bullet} \rightarrow H_2O_2 + O_2\ (SOD) \quad (5)$$

Whereas MitoQ increased complex I–driven mitochondrial H_2O_2 production and complex II–driven mitochondrial H_2O_2 production in the presence of rotenone, CoQ_{10} did not. The ability of CoQ_{10} to act as an electron carrier and restore respiration in CoQ-deficient yeast with its fast oxidation by complex III is consistent with the fact that CoQ_{10} did not promote aberrant electron leakage to molecular oxygen in our experiments. In contrast, MitoQ cannot act as an electron carrier or restore respiration because it is not oxidized by complex III (13). We speculate that once it is reduced, the only pathway through which MitoQ recycles back to its oxidized quinone form is by transferring its electrons to molecular oxygen, leading to the formation of $O_2^{\bullet}$. Furthermore, the prooxidant effects of MitoQ can potentially be explained by the fact that its large hydrophilic and positively charged core remains in the aqueous phase. The deprotonation of the reduced form of MitoQ is chemically favored in the aqueous environment. Once deprotonated, it will lead to an oxidation reaction of quinol, producing $O_2^{\bullet}$. This is in marked contrast to the native ubiquinone, which is freely soluble within the mitochondrial lipid membrane. A quinol within a phospholipid bilayer is unlikely to be oxidized by this pathway (13, 14). This offers an additional plausible explanation why ROS production occurs only with MitoQ but not with CoQ_{10}.

Mitoquinone prooxidant effects were also observed in mitochondria isolated from endothelial cells treated with MitoQ for 1 h. It is noteworthy that the levels of ROS production by mitochondria in this case were substantially higher than those observed in isolated mitochondria treated acutely with increasing concentrations of MitoQ. These findings are consistent with the observation that MitoQ is indeed accumulating within mitochondria, where it redox cycles.

These changes in mitochondrial function had a significant effect on endothelial cell ROS production and survival, as is evidenced by the fact that MitoQ significantly increased endothelial $O_2^{\bullet}$ levels and caspase-3 activity. Mitochondrial oxidative stress carries detrimental consequences on cellular survival. It is well known that mitochondrial damage leads to cytochrome *c* release, caspase activation, and ultimately, apoptosis (2). MitoQ did lead to cellular apoptosis when applied in 0.1 and 1 μM concentrations in BAECs. This effect was most pronounced at 4-h incubation, at which time we started observing apoptotic changes in incubated cells.

Thus, we conclude that MitoQ increases mitochondrial as well as cellular ROS production because of its redox cycling properties, as demonstrated in a cell-free system by using cytochrome P450 reductase, in intact endothelial cells, and mitochondria treated acutely with the drug or isolated from cells after prior 1-h exposure, as well as submitochondrial particles and purified complex I fueled with NADH. This increase in oxidative stress resulted in caspase 3 activation and cellular apoptosis. We also suggest two sites of redox cycling in mitochondria, which are most likely at the level of the reduced flavin and bound UQ groups in complex I, as evidenced by the use of rotenone or stigmatellin or both in intact mitochondria, in addition to our experiments with SMP and purified complex I (Fig. 8). Use of MitoQ as a mitochondrial antioxidant should be interpreted with caution, even at very low concentrations. Other drugs, such as mitochondrially targeted nitroxides that lack a quinone moiety and are unable to generate $O_2^{\bullet}$, may prove

to be more effective in protecting mitochondrial function against oxidative damage (6).

ACKNOWLEDGMENTS

We are indebted to Dr. Jay Joseph for providing us with mitoquinone. This work was supported by funding from National Institutes of Health grants PO-1 HL058000 and PO-1 HL075209, and by the American Heart Association SDG 0430201N.

ABBREVIATIONS

AAP, 4-acetamidophenol; αKG, α-ketoglutarate; αKGDH, α-ketoglutarate dehydrogenase complex; BAECs, bovine aortic endothelial cells; CAT1H, 1-hydroxy-2,2,6,6-tetramethylpiperidin-4-yl-trimethylammonium; CoQ_{10}, ubiquinone-10; COX, cytochrome oxidase; EMPO, 2-ethoxycarbonyl-2-methyl-3,4-dihydro-2*H*-pyrrole-1-oxide; ESR, electron spin resonance; FMN, flavin-mononucleotide; GAPDH; glyceraldehyde-3-phosphate dehydrogenase; HPLC, high-performance liquid chromatography; HRP, horseradish peroxidase; H_2O_2, hydrogen peroxide; LM, *n*-dodecyl-β-D-maltoside; MitoQ, mitoquinone; $O_2^{\bullet-}$, superoxide; QH_2, ubiquinol; ROS, reactive oxygen species; SOD, superoxide dismutase; UQ, ubiquinone.

REFERENCES

1. Adam-Vizi V. Production of reactive oxygen species in brain mitochondria: contribution by electron transport chain and non-electron transport chain sources. *Antioxid Redox Signal* 7: 1140–1149, 2005.
2. Anuradha CD, Kanno S, and Hirano S. Oxidative damage to mitochondria is a preliminary step to caspase-3 activation in fluoride-induced apoptosis in HL-60 cells. *Free Radic Biol Med* 31: 367–373, 2001.
3. Buettner GR, Ng CF, Wang M, Rodgers VG, and Schafer FQ. A new paradigm: manganese superoxide dismutase influences the production of H_2O_2 in cells and thereby their biological state. *Free Radic Biol Med* 41: 1338–1350, 2006.
4. Cadenas E and Davies KJ. Mitochondrial free radical generation, oxidative stress, and aging. *Free Radic Biol Med* 29: 222–230, 2000.
5. Dhanasekaran A, Kotamraju S, Kalivendi SV, Matsunaga T, Shang T, Keszler A, Joseph J, and Kalyanaraman B. Supplementation of endothelial cells with mitochondria-targeted antioxidants inhibit peroxide-induced mitochondrial iron uptake, oxidative damage, and apoptosis. *J Biol Chem* 279: 37575–37587, 2004.
6. Dhanasekaran A, Kotamraju S, Karunakaran C, Kalivendi SV, Thomas S, Joseph J, and Kalyanaraman B. Mitochondria superoxide dismutase mimetic inhibits peroxide-induced oxidative damage and apoptosis: role of mitochondrial superoxide. *Free Radic Biol Med* 39: 567–583, 2005.
7. Dikalov S, Landmesser U, and Harrison DG. Geldanamycin leads to superoxide formation by enzymatic and non-enzymatic redox cycling: implications for studies of Hsp90 and endothelial cell nitric-oxide synthase. *J Biol Chem* 277: 25480–25485, 2002.
8. Esplugues JV, Rocha M, Nunez C, Bosca I, Ibiza S, Herance JR, Ortega A, Serrador JM, D'Ocon P, and Victor VM. Complex I dysfunction and tolerance to nitroglycerin: an approach based on mitochondrial-targeted antioxidants. *Circ Res* 99: 1067–1075, 2006.
9. Fink B, Laude K, McCann L, Doughan A, Harrison DG, and Dikalov S. Detection of intracellular superoxide formation in endothelial cells and intact tissues using dihydroethidium and an HPLC-based assay. *Am J Physiol Cell Physiol* 287: C895–C902, 2004.
10. Genova ML, Pich MM, Bernacchia A, Bianchi C, Biondi A, Bovina C, Falasca AI, Formiggini G, Castelli GP, and Lenaz G. The mitochondrial production of reactive oxygen species in relation to aging and pathology. *Ann N Y Acad Sci* 1011: 86–100, 2004.
11. Gibson GE, Blass JP, Beal MF, and Bunik V. The alpha-ketoglutarate-dehydrogenase complex: a mediator between mitochondria and oxidative stress in neurodegeneration. *Mol Neurobiol* 31: 43–63, 2005.
12. Grivennikova VG and Vinogradov AD. Generation of superoxide by the mitochondrial complex I. *Biochim Biophys Acta* 1757: 553–561, 2006.
13. James AM, Cocheme HM, Smith RA, and Murphy MP. Interactions of mitochondria-targeted and untargeted ubiquinones with the mitochondrial respiratory chain and reactive oxygen species: implications for the use of exogenous ubiquinones as therapies and experimental tools. *J Biol Chem* 280: 21295–21312, 2005.
14. James AM, Smith RA, and Murphy MP. Antioxidant and prooxidant properties of mitochondrial coenzyme Q. *Arch Biochem Biophys* 423: 47–56, 2004.
15. Keeney PM, Xie J, Capaldi RA, and Bennett JP Jr. Parkinson's disease brain mitochondrial complex I has oxidatively damaged subunits and is functionally impaired and misassembled. *J Neurosci* 26: 5256–5264, 2006.
16. Kelso GF, Porteous CM, Coulter CV, Hughes G, Porteous WK, Ledgerwood EC, Smith RA, and Murphy MP. Selective targeting of a redox-active ubiquinone to mitochondria within cells: antioxidant and antiapoptotic properties. *J Biol Chem* 276: 4588–4596, 2001.
17. Kelso GF, Porteous CM, Hughes G, Ledgerwood EC, Gane AM, Smith RA, and Murphy MP. Prevention of mitochondrial oxidative damage using targeted antioxidants. *Ann N Y Acad Sci* 959: 263–274, 2002.
18. Khatri JJ, Johnson C, Magid R, Lessner SM, Laude KM, Dikalov SI, Harrison DG, Sung HJ, Rong Y, and Galis ZS. Vascular oxidant stress enhances progression and angiogenesis of experimental atheroma. *Circulation* 109: 520–525, 2004.
19. Kussmaul L and Hirst J. The mechanism of superoxide production by NADH:ubiquinone oxidoreductase (complex I) from bovine heart mitochondria. *Proc Natl Acad Sci U S A* 103: 7607–7612, 2006.
20. McManus DC and Josephy PD. A new approach to measurement of redox-cycling activity in *Escherichia coli*. *Arch Biochem Biophys* 304: 367–370, 1993.
21. Moreno-Sanchez R, Covian R, Jasso-Chavez R, Rodriguez-Enriquez S, Pacheco-Moises F, and Torres-Marquez ME. Oxidative phosphorylation supported by an alternative respiratory pathway in mitochondria from *Euglena*. *Biochim Biophys Acta* 1457: 200–210, 2000.
22. Mukherjee TK, Mishra AK, Mukhopadhyay S, and Hoidal JR. High concentration of antioxidants N-acetylcysteine and mitoquinone-q induces intercellular adhesion molecule 1 and oxidative stress by increasing intracellular glutathione. *J Immunol* 178: 1835–1844, 2007.
23. O'Malley Y, Fink BD, Ross NC, Prisinzano TE, and Sivitz WI. Reactive oxygen and targeted antioxidant administration in endothelial cell mitochondria. *J Biol Chem* 281: 39766–39775, 2006.
24. Ohnishi ST, Ohnishi T, Muranaka S, Fujita H, Kimura H, Uemura K, Yoshida K, and Utsumi K. A possible site of superoxide generation in the complex I segment of rat heart mitochondria. *J Bioenerg Biomembr* 37: 1–15, 2005.
25. Panov A, Dikalov S, Shalbuyeva N, Taylor G, Sherer T, and Greenamyre JT. Rotenone model of Parkinson disease: multiple brain mitochondria dysfunctions after short term systemic rotenone intoxication. *J Biol Chem* 280: 42026–42035, 2005.
26. Panov AV, Lund S, and Greenamyre JT. Ca^{2+}-induced permeability transition in human lymphoblastoid cell mitochondria from

normal and Huntington's disease individuals. *Mol Cell Biochem* 269: 143–152, 2005.
27. Sazanov LA and Hinchliffe P. Structure of the hydrophilic domain of respiratory complex I from *Thermus thermophilus*. *Science* 311: 1430–1436, 2006.
28. Skulachev VP. How to clean the dirtiest place in the cell: cationic antioxidants as intramitochondrial ROS scavengers. *IUBMB Life* 57: 305–310, 2005.
29. Starkov AA, Fiskum G, Chinopoulos C, Lorenzo BJ, Browne SE, Patel MS, and Beal MF. Mitochondrial alpha-ketoglutarate dehydrogenase complex generates reactive oxygen species. *J Neurosci* 24: 7779–7788, 2004.
30. Yorek MA. The role of oxidative stress in diabetic vascular and neural disease. *Free Radic Res* 37: 471–480, 2003.

Address reprint requests to:
Sergey I. Dikalov, Ph.D.
Emory University School of Medicine
Division of Cardiology
101 Woodruff Circle, Suite 319 WMB
Atlanta, GA 30322

E-mail: dikalov@emory.edu

Date of first submission to ARS Central, April 6, 2007; date of final revised submission, June 25, 2007; date of acceptance, June 26, 2007.

This article has been cited by:

1. Jan Gruber, Sheng Fong, Ce-Belle Chen, Sialee Yoong, Giorgia Pastorin, Sebastian Schaffer, Irwin Cheah, Barry Halliwell. 2012. Mitochondria-targeted antioxidants and metabolic modulators as pharmacological interventions to slow ageing. *Biotechnology Advances* . [CrossRef]
2. Nicola Sassi, Lucia Biasutto, Andrea Mattarei, Massimo Carraro, Valentina Giorgio, Anna Citta, Paolo Bernardi, Spiridione Garbisa, Ildikò Szabò, Cristina Paradisi, Mario Zoratti. 2012. Cytotoxicity of a mitochondriotropic quercetin derivative: Mechanisms. *Biochimica et Biophysica Acta (BBA) - Bioenergetics* **1817**:7, 1095-1106. [CrossRef]
3. V. P. Skulachev. 2012. What is “phenoptosis” and how to fight it?. *Biochemistry (Moscow)* **77**:7, 689-706. [CrossRef]
4. Dao-Fu Dai , Tony Chen , Simon C. Johnson , Hazel Szeto , Peter S. Rabinovitch . 2012. Cardiac Aging: From Molecular Mechanisms to Significance in Human Health and Disease. *Antioxidants & Redox Signaling* **16**:12, 1492-1526. [Abstract] [Full Text HTML] [Full Text PDF] [Full Text PDF with Links]
5. Robin Smith, Richard Hartley, Michael MurphyMitochondria-Targeted Antioxidants **30**, 111-114. [CrossRef]
6. Robin A.J. Smith , Richard C. Hartley , Michael P. Murphy . 2011. Mitochondria-Targeted Small Molecule Therapeutics and Probes. *Antioxidants & Redox Signaling* **15**:12, 3021-3038. [Abstract] [Full Text HTML] [Full Text PDF] [Full Text PDF with Links]
7. Sergey Dikalov. 2011. Cross talk between mitochondria and NADPH oxidases. *Free Radical Biology and Medicine* . [CrossRef]
8. M. N. Yurova, M. A. Zabezhinski, T. S. Piskunova, M. L. Tyndyk, I. G. Popovich, V. N. Anisimov. 2011. Effect of mitochondria-targeted antioxidant SkQ1 on aging, lifespan, and spontaneous carcinogenesis in three strains of mice. *Advances in Gerontology* **1**:3, 260-271. [CrossRef]
9. Francesco Visioli, Catalina Alarcón De La Lastra, Cristina Andres-Lacueva, Michael Aviram, Conceição Calhau, Alfredo Cassano, Massimo D’Archivio, Ana Faria, Gaëlle Favé, Vincenzo Fogliano, Rafael Llorach, Paola Vitaglione, Mario Zoratti, Marvin Edeas. 2011. Polyphenols and Human Health: A Prospectus. *Critical Reviews in Food Science and Nutrition* **51**:6, 524-546. [CrossRef]
10. Barry Halliwell. 2011. Free radicals and antioxidants – quo vadis?. *Trends in Pharmacological Sciences* **32**:3, 125-130. [CrossRef]
11. F. F. Severin, V. P. Skulachev. 2011. Programmed cell death as a target to interrupt the aging program. *Advances in Gerontology* **1**:1, 16-27. [CrossRef]
12. Sangbin Lim, Md Abdur Rashid, Miran Jang, Yeonghwan Kim, Hyeran Won, Jeonghoon Lee, Jeong-taek Woo, Young Seol Kim, Michael P. Murphy, Liaquat Ali, Joohun Ha, Sung Soo Kim. 2011. Mitochondria-targeted Antioxidants Protect Pancreatic #-cells against Oxidative Stress and Improve Insulin Secretion in Glucotoxicity and Glucolipotoxicity. *Cellular Physiology and Biochemistry* **28**:5, 873-886. [CrossRef]
13. Anamitra Ghosh, Karunakaran Chandran, Shasi V. Kalivendi, Joy Joseph, William E. Antholine, Cecilia J. Hillard, Arthi Kanthasamy, Anumantha Kanthasamy, Balaraman Kalyanaraman. 2010. Neuroprotection by a mitochondria-targeted drug in a Parkinson's disease model. *Free Radical Biology and Medicine* **49**:11, 1674-1684. [CrossRef]
14. S. M. Davidson. 2010. Endothelial mitochondria and heart disease. *Cardiovascular Research* **88**:1, 58-66. [CrossRef]
15. Robin A.J. Smith, Michael P. Murphy. 2010. Animal and human studies with the mitochondria-targeted antioxidant MitoQ. *Annals of the New York Academy of Sciences* **1201**:1, 96-103. [CrossRef]
16. V. P. Skulachev. 2010. How to cancel the program of body aging?. *Russian Journal of General Chemistry* **80**:7, 1523-1541. [CrossRef]
17. Werner J.H. Koopman , Leo G.J. Nijtmans , Cindy E.J. Dieteren , Peggy Roestenberg , Federica Valsecchi , Jan A.M. Smeitink , Peter H.G.M. Willems . 2010. Mammalian Mitochondrial Complex I: Biogenesis, Regulation, and Reactive Oxygen Species Generation. *Antioxidants & Redox Signaling* **12**:12, 1431-1470. [Abstract] [Full Text HTML] [Full Text PDF] [Full Text PDF with Links]
18. Vladimir P. Skulachev, Yury N. Antonenko, Dmitry A. Cherepanov, Boris V. Chernyak, Denis S. Izyumov, Ludmila S. Khailova, Sergey S. Klishin, Galina A. Korshunova, Konstantin G. Lyamzaev, Olga Yu. Pletjushkina, Vitaly A. Roginsky, Tatiana I. Rokitskaya, Fedor F. Severin, Inna I. Severina, Ruben A. Simonyan, Maxim V. Skulachev, Natalia V. Sumbatyan, Evgeniya I. Sukhanova, Vadim N. Tashlitsky, Tatyana A. Trendeleva, Mikhail Yu. Vyssokikh, Renata A. Zvyagilskaya. 2010. Prevention of cardiolipin oxidation and fatty acid cycling as two antioxidant mechanisms of cationic derivatives of plastoquinone (SkQs). *Biochimica et Biophysica Acta (BBA) - Bioenergetics* **1797**:6-7, 878-889. [CrossRef]

19. William I. Sivitz , Mark A. Yorek . 2010. Mitochondrial Dysfunction in Diabetes: From Molecular Mechanisms to Functional Significance and Therapeutic Opportunities. *Antioxidants & Redox Signaling* **12**:4, 537-577. [Abstract] [Full Text HTML] [Full Text PDF] [Full Text PDF with Links]
20. Judy A. Herlein, Brian D. Fink, William I. Sivitz. 2010. Superoxide production by mitochondria of insulin-sensitive tissues: mechanistic differences and effect of early diabetes. *Metabolism* **59**:2, 247-257. [CrossRef]
21. F. F. Severin, I. I. Severina, Y. N. Antonenko, T. I. Rokitskaya, D. A. Cherepanov, E. N. Mokhova, M. Y. Vyssokikh, A. V. Pustovidko, O. V. Markova, L. S. Yaguzhinsky, G. A. Korshunova, N. V. Sumbatyan, M. V. Skulachev, V. P. Skulachev. 2010. Penetrating cation/fatty acid anion pair as a mitochondria-targeted protonophore. *Proceedings of the National Academy of Sciences* **107**:2, 663-668. [CrossRef]
22. Sergio Rodriguez-Cuenca, Helena M. Cochemé, Angela Logan, Irina Abakumova, Tracy A. Prime, Claudia Rose, Antonio Vidal-Puig, Anthony C. Smith, David C. Rubinsztein, Ian M. Fearnley, Bruce A. Jones, Simon Pope, Simon J.R. Heales, Brian Y.H. Lam, Sudeshna Guha Neogi, Ian McFarlane, Andrew M. James, Robin A.J. Smith, Michael P. Murphy. 2010. Consequences of long-term oral administration of the mitochondria-targeted antioxidant MitoQ to wild-type mice. *Free Radical Biology and Medicine* **48**:1, 161-172. [CrossRef]
23. Umberto De Marchi, Lucia Biasutto, Spiridione Garbisa, Antonio Toninello, Mario Zoratti. 2009. Quercetin can act either as an inhibitor or an inducer of the mitochondrial permeability transition pore: A demonstration of the ambivalent redox character of polyphenols. *Biochimica et Biophysica Acta (BBA) - Bioenergetics* **1787**:12, 1425-1432. [CrossRef]
24. Natalia A. Belikova, Ashley Glumac, Ruslan Rafikov, Jianfei Jiang, Joel S. Greenberger, Valerian E. Kagan, Hülya Bayir. 2009. Radioprotection by short-term oxidative preconditioning: Role of manganese superoxide dismutase. *FEBS Letters* **583**:21, 3437-3442. [CrossRef]
25. Jan Gruber, Li Fang Ng, Suresh Kumar Poovathingal, Barry Halliwell. 2009. Deceptively simple but simply deceptive – Caenorhabditis elegans lifespan studies: Considerations for aging and antioxidant effects. *FEBS Letters* **583**:21, 3377-3387. [CrossRef]
26. Huan Ling Liang, Jody Arsenault, Jordan Mortensen, Frank Park, Christopher P. Johnson, Vani Nilakantan. 2009. Partial attenuation of cytotoxicity and apoptosis by SOD1 in ischemic renal epithelial cells. *Apoptosis* **14**:10, 1176-1189. [CrossRef]
27. Lydie Plecitá-Hlavatá, Jan Ježek, Petr Ježek. 2009. Pro-oxidant mitochondrial matrix-targeted ubiquinone MitoQ10 acts as anti-oxidant at retarded electron transport or proton pumping within Complex I. *The International Journal of Biochemistry & Cell Biology* **41**:8-9, 1697-1707. [CrossRef]
28. Vladimir P. Skulachev, Vladimir N. Anisimov, Yuri N. Antonenko, Lora E. Bakeeva, Boris V. Chernyak, Valery P. Erichev, Oleg F. Filenko, Natalya I. Kalinina, Valery I. Kapelko, Natalya G. Kolosova. 2009. An attempt to prevent senescence: A mitochondrial approach. *Biochimica et Biophysica Acta (BBA) - Bioenergetics* **1787**:5, 437-461. [CrossRef]
29. Jacek Zielonka, Micael Hardy, B. Kalyanaraman. 2009. HPLC study of oxidation products of hydroethidine in chemical and biological systems: ramifications in superoxide measurements. *Free Radical Biology and Medicine* **46**:3, 329-338. [CrossRef]
30. Amy Y. Tsou, Lisa S. Friedman, Robert B. Wilson, David R. Lynch. 2009. Pharmacotherapy for Friedreich Ataxia. *CNS Drugs* **23**:3, 213-223. [CrossRef]
31. Tiffany J. Somers-Edgar, Rhonda J. Rosengren. 2009. Coenzyme Q0 induces apoptosis and modulates the cell cycle in estrogen receptor negative breast cancer cells. *Anti-Cancer Drugs* **20**:1, 33-40. [CrossRef]
32. Y. N. Antonenko, A. V. Avetisyan, L. E. Bakeeva, B. V. Chernyak, V. A. Chertkov, L. V. Domnina, O. Yu. Ivanova, D. S. Izyumov, L. S. Khailova, S. S. Klishin, G. A. Korshunova, K. G. Lyamzaev, M. S. Muntyan, O. K. Nepryakhina, A. A. Pashkovskaya, O. Yu. Pletjushkina, A. V. Pustovidko, V. A. Roginsky, T. I. Rokitskaya, E. K. Ruuge, V. B. Saprunova, I. I. Severina, R. A. Simonyan, I. V. Skulachev, M. V. Skulachev, N. V. Sumbatyan, I. V. Sviryaeva, V. N. Tashlitsky, J. M. Vassiliev, M. Yu. Vyssokikh, L. S. Yaguzhinsky, A. A. Zamyatnin, V. P. Skulachev. 2008. Mitochondria-targeted plastoquinone derivatives as tools to interrupt execution of the aging program. 1. Cationic plastoquinone derivatives: Synthesis and in vitro studies. *Biochemistry (Moscow)* **73**:12, 1273-1287. [CrossRef]
33. Paule Bénit, Abdelhamid Slama, Pierre Rustin. 2008. Decylubiquinol impedes mitochondrial respiratory chain complex I activity. *Molecular and Cellular Biochemistry* **314**:1-2, 45-50. [CrossRef]
34. Magnus Bentinger, Michael Tekle, Kerstin Brismar, Tadeusz Chojnacki, Ewa Swiezewska, Gustav Dallner. 2008. Stimulation of coenzyme Q synthesis. *BioFactors* **32**:1-4, 99-111. [CrossRef]